

# The role of disc self-gravity in the formation of protostars and protostellar discs

W.K.M. Rice<sup>1\*</sup>, J.H. Mayo<sup>1</sup>, Philip J. Armitage<sup>2,3</sup>

<sup>1</sup> *SUPA†, Institute for Astronomy, University of Edinburgh, Blackford Hill, Edinburgh, EH9 3HJ*

<sup>2</sup> *JILA, Campus Box 440, University of Colorado, Boulder CO 80309*

<sup>3</sup> *Department of Astrophysical and Planetary Sciences, University of Colorado, Boulder CO 80309*

11 October 2021

## ABSTRACT

We use time-dependent, one-dimensional disc models to investigate the evolution of protostellar discs that form through the collapse of molecular cloud cores and in which the primary transport mechanism is self-gravity. We assume that these discs settle into a state of thermal equilibrium with  $Q = 2$  and that the strength of the angular momentum transport is set by the cooling rate of the disc. The results suggest that these discs will attain a quasi-steady state that persists for a number of free-fall times and in which most of the mass within 100 au is located inside 10–20 au. This pile-up of mass in the inner disc could result in temperatures that are high enough for the growth of MHD turbulence which could rapidly drain the inner disc and lead to FU Orionis-like outbursts. In all our simulations, the inner regions of the discs ( $r < 40$  au) were stable against fragmentation, while fragmentation was possible in the outer regions ( $r > 40$  au) of discs that formed from cores that had enough initial angular momentum to deposit sufficient mass in these outer regions. The large amounts of mass in these outer regions, however, suggests that fragmentation will lead to the formation of substellar and stellar mass companions, rather than planetary mass objects. Although mass accretion rates were largely consistent with observations, the large disc masses suggest that an additional transport mechanism (such as MRI occurring in the upper layers of the disc) must operate in order to drain the remaining disc material within observed disc lifetimes.

**Key words:** stars: formation — stars: pre-main-sequence — circumstellar matter — planetary systems: protoplanetary discs — planetary systems: formation

## 1 INTRODUCTION

The formation of low-mass stars occurs through the collapse of cold, dense molecular cloud cores (Terebey, Shu & Cassen 1984). These cores, however, generally contain amounts of angular momentum far in excess of the rotational angular momentum of a single star (Caselli et al. 2002). Most of the mass must therefore first pass through a circumstellar disc before accreting onto the central star. One of the open problems in star and planet formation is what mechanism acts to transport the angular momentum outwards, allowing this accretion to take place.

It is now generally accepted that in most astrophysical discs, angular momentum transport is driven by magnetohydrodynamic (MHD) turbulence initiated by the magneto-rotational instability (MRI) (Balbus & Hawley

1991; Papaloizou & Nelson 2003). During the earliest stages of star formation protoplanetary discs are, however, cold and dense and probably do not have even the very small degree of ionization needed to sustain MHD turbulence (Blaes & Balbus 1994). At these early times, the disc is, however, likely to be massive and disc self-gravity may then provide an alternate and possibly dominant transport mechanism through the growth of the gravitational instability (Toomre 1964; Lin & Pringle 1987; Laughlin & Bodenheimer 1994).

Although it has been suggested that gravitationally unstable discs may fragment to form gas giant planets or substellar companions (Boss 1998, 2002), it is now generally accepted that the conditions for fragmentation are difficult to achieve in the inner planet forming regions of protostellar discs (Matzner & Levin 2005; Rafikov 2005; Boley et al. 2006; Whitworth & Stamatellos 2006; Stamatellos & Whitworth 2008; Forgan et al. 2009). A self-

\* E-mail: wkmr@roe.ac.uk

† Scottish Universities Physics Alliance

gravitating protostellar disc is more likely to settle into a quasi-steady state in which the instability acts to transport angular momentum outwards (Gammie 2001; Rice et al. 2003; Lodato & Rice 2004; Vorobyov & Basu 2007). It has been shown (Lodato & Rice 2004, 2005) that in this quasi-steady state, the transport can be approximated as a local viscous process for all but the most massive discs. Since the disc will also be in thermal equilibrium, the strength of the angular momentum transport is also set by the cooling rate of the disc (Gammie 2001; Rice et al. 2003). Using the above results, Rice & Armitage (2009) have shown that if self-gravity is the dominant transport mechanism, protostellar discs will settle into quasi-steady states that are largely independent of the initial conditions. The resulting surface density profiles are quite steep with  $\sim 80\%$  of the mass within 50 au located inside 10–20 au. Rice & Armitage (2009) also found that the quasi-steady mass accretion rates depend strongly on the disc mass and on the mass of the central star. Their simulations also suggested that no regions of the disc (which extended to 50 au) were susceptible to fragmentation with the inner 10 – 20 au being particularly stable, consistent with other recent calculations (Clarke 2009; Rafikov 2009).

The simulations carried out by Rice & Armitage (2009) assumed initial power-law surface density profiles that were evolved until a quasi-steady state - which we define as a state in which the mass accretion rate is approximately independent of radius - was achieved. Although this gives information about the quasi-steady nature of such systems, it doesn't tell us if such a state can be achieved under realistic conditions. Here, we extend the work of Rice & Armitage (2009) by considering the evolution of self-gravitating, circumstellar discs formed through infall from a molecular cloud core. We find that these discs do settle rapidly into quasi-steady states, with properties similar to that found by Rice & Armitage (2009). The mass accretion rates are also generally consistent with observations (Muzerolle et al. 2005), although at early times the simulated accretion rates are somewhat higher than observed. Although the disc masses are generally higher than observed, a significant fraction of the mass is located in the optically thick inner regions and would not be easily detected using current techniques. These results are consistent with the suggestion (Armitage, Livio & Pringle 2001; Zhu, Hartmann & Gammie 2009) that mass will pile-up in the inner regions of the disc and will drain episodically onto the star - potentially explaining FU Orionis outbursts (Hartmann & Kenyon 1996) - when the temperature becomes sufficiently high for MRI to operate.

The paper is organised as follows. In Section 2, we describe the basic model that builds the disc from an infalling molecular cloud core and evolves the disc self-consistently through, primarily, self-gravity. In Section 3, we describe the results, and in Section 4 we summarize our conclusions.

## 2 BASIC MODEL

### 2.1 Infall

We base the model here on that of Lin & Pringle (1990) which itself is based on the earlier work of

Cassen & Moosman (1981). We consider a molecular cloud core of mass  $M_c$ , radius  $R_c$  and angular velocity  $\Omega_c$  that is assumed to have an initially uniform density,  $\rho_c$ . The core is allowed to collapse under gravity, with the collapse occurring on a characteristic free-fall time of  $t_{\text{ff}} = (3\pi/32G\rho_c)^{1/2}$ . As in Lin & Pringle (1990), we assume that the collapse is initially steady (Larson 1969) and then, after one free-fall time, decreases smoothly to zero over a further free-fall time. The form of the accretion rate is therefore (Lin & Pringle 1990)

$$\dot{M}(t) = \begin{cases} \frac{M_c}{t_{\text{ff}}} & 0 \leq t \leq t_{\text{ff}} \\ \frac{1}{2} \frac{M_c}{t_{\text{ff}}} \left[ 1 + \cos \frac{\pi(t-t_{\text{ff}})}{t_{\text{ff}}} \right] & t_{\text{ff}} \leq t \leq 2t_{\text{ff}} \\ 0 & 2t_{\text{ff}} \leq t \end{cases}, \quad (1)$$

which implies that the total amount of mass accreted is actually  $1.5M_c$ . The infalling material is assumed to conserve angular momentum and consequently produces a centrifugally supported disc which, in the absence of angular momentum transport, would have a maximum radius of  $a_{\text{max}} = \Omega_c^2 R_c^4 / GM_c$ . We model the infall (Cassen & Moosman 1981) as the collapse of shells with each part of a shell striking the disc plane at the same time. The fraction of the mass of a shell, with initial radius  $r_o$  and enclosed mass  $M(< r_o)$ , that strikes the disc within radius  $r$  is (Lin & Pringle 1990)

$$g(r) = 1 - \left( 1 - \frac{r}{a_o} \right)^{1/2} \quad 0 \leq r \leq a_o, \quad (2)$$

where

$$a_o = \frac{\Omega_c^2 r_o^4}{GM(< r_o)}. \quad (3)$$

At  $t = 0$  the initial timestep,  $dt$ , determines, through equation (1), the amount of mass added and hence the amount of mass in the current shell. Since the core is assumed to have a uniform density,  $\rho_c$ , this determines the radial extent of the initial shell. Equation (2), together with equation (3), then determines how the mass in the shell is distributed in the disc. In subsequent timesteps, the radial extent of the next shell is then determined by ensuring that the amount of mass in the shell matches the amount of mass being added in that timestep, and the mass in that shell is distributed in the same way as in the first timestep.

### 2.2 Disc evolution

In order for the disc to evolve there needs to be some mechanism for transporting angular momentum outwards, allowing mass to accrete onto the central star. Generally this is assumed to take the form of some kind of kinematic viscosity,  $\nu$ , which would cause an axisymmetric disc of surface density  $\Sigma(R, t)$  to evolve as (Lynden-Bell & Pringle 1974; Pringle 1981)

$$\frac{\partial \Sigma}{\partial t} = \frac{3}{r} \frac{\partial}{\partial r} \left[ r^{1/2} \frac{\partial}{\partial r} \left( \nu \Sigma r^{1/2} \right) \right]. \quad (4)$$

In the work of Lin & Pringle (1990) the kinematic viscosity is assumed to be the sum of two components. The first component is a standard ‘‘turbulent’’ viscosity given by

$$\nu_{\text{ss}} = \alpha_{\text{ss}} \frac{c_s^2}{\Omega}, \quad (5)$$

where  $c_s$  is the disc sound speed,  $\Omega$  is the angular frequency, and  $\alpha_{\text{ss}} \ll 1$  is a parameter that determines the efficiency

of the angular momentum transport (Shakura & Sunyaev 1973). In astrophysical discs, the mechanism that provides this kinematic viscosity is generally accepted to be magneto-hydrodynamic (MHD) turbulence initiated by the magneto-rotational instability (Balbus & Hawley 1991). The second component,  $\nu_g$ , was only non-zero if the disc was self-gravitating.

An accretion disc can become gravitational unstable if (Toomre 1964)

$$Q = \frac{c_s \kappa}{\pi G \Sigma} \sim 1, \quad (6)$$

where  $\kappa$  is the epicyclic frequency and can be replaced by the angular frequency,  $\Omega$ , in a Keplerian disc. Following Lin & Pringle (1987), Lin & Pringle (1990) assumed that  $\nu_g$  was zero unless  $Q \leq Q_c$ , where  $Q_c$  was a critical value below which the disc became gravitationally unstable, and that  $\nu_g$  increased as  $Q$  decreased. The evolution of self-gravitating discs has, however, been studied in quite some detail recently (Gammie 2001; Rice et al. 2003; Lodato & Rice 2004; Mejia et al. 2005; Durisen et al. 2007) and it is now generally thought that such discs will tend to settle into a state with constant  $Q$  and in which the heating and cooling rates balance.

This work therefore differs from Lin & Pringle (1990) in two ways. We firstly assume - at least during the earliest phases of star formation - that in general the disc is too cold and dense to have even the small degree of ionization needed to sustain MHD turbulence (Blaes & Balbus 1994). In this case  $\alpha_{ss} = 0$  and disc self-gravity is the dominant mechanism for transporting angular momentum. We secondly assume that the disc will quickly settle into quasi-steady state with  $Q \sim 2$ . In this state the disc is assumed to be in thermal equilibrium with the radiative cooling balanced by heating occurring primarily through compressions and shocks. If we assume that the energy is dissipated locally, which appears to be the case when  $Q \sim 1$  (Balbus & Papaloizou 1999; Lodato & Rice 2004), the dissipation is equivalent to that occurring through an effective gravitational viscosity. Matching the dissipation rate with the known cooling rate allows the effective gravitational  $\alpha$  to be determined (Rice & Armitage 2009) and the disc is then evolved using equation (4).

### 2.3 Determining the effective gravitational viscosity

If we assume that a quasi-steady, self-gravitating disc introduces an effective gravitational viscosity,  $\nu_g$ , the dissipation in the disc,  $D(R)$ , per unit area per unit time is (Bell & Lin 1994)

$$D(R) = \frac{9}{4} \nu_g \Sigma \Omega^2. \quad (7)$$

To determine the cooling rate we need to know the midplane temperature and the optical depth. The midplane temperature can be determined using

$$T_c = \frac{\mu m_p c_s^2}{\gamma k_B}, \quad (8)$$

where  $\mu = 2.4$  is the mean molecular weight,  $m_p$  is the proton mass,  $\gamma = 1.4$  is the specific heat ratio,  $k_B$  is Boltzmann's constant, and  $c_s$  is the sound speed determined from

the condition that  $Q = 2$ . We have the additional constraint that  $T_c$  cannot be less than 10 K. We approximate the optical depth using

$$\tau = \int_0^\infty dz \kappa(\rho_z, T_z) \rho_z \approx H \kappa(\bar{\rho}, \bar{T}) \bar{\rho}, \quad (9)$$

where  $\kappa$  is the Rosseland mean opacity and  $\bar{\rho}$  and  $\bar{T}$  are an average density and temperature for which we use  $\bar{\rho} = \Sigma/(2H)$  and  $\bar{T} = T_c$ . The Rosseland mean opacities are determined using the analytic approximations from Bell & Lin (1994). Once the optical depth is known, the cooling function,  $\Lambda$ , can be approximated using (Hubeny 1990)

$$\Lambda = \frac{16\sigma}{3} (T_c^4 - T_o^4) \frac{\tau}{1 + \tau^2}, \quad (10)$$

where  $T_o = 10$  K is an assumed minimum temperature set by some background sources (Stamatellos et al. 2007), and the last term is introduced to smoothly interpolate between optically thick and optically thin regions (Johnson & Gammie 2003). The effective gravitational viscosity can then be determined by equating equations (7) and (10). If, however, we rewrite the gravitational viscosity as  $\nu_g = \alpha_g c_s^2 / \Omega$  and use that  $t_{cool} = U/\Lambda$ , where  $U$  is the internal energy per unit area given by

$$U = \frac{c_s^2 \Sigma}{\gamma(\gamma - 1)}, \quad (11)$$

we get (Gammie 2001)

$$\alpha_g = \frac{4}{9\gamma(\gamma - 1)t_{cool}\Omega}. \quad (12)$$

Although we are assuming that the primary transport mechanism is self-gravity, if regions of the disc were hot enough to be partially ionised, MRI may play a role in these regions. We therefore assume that if the temperature exceeds  $\sim 1400$  K MRI will operate and set  $\alpha = \alpha_{ss} + \alpha_g = 0.01$ . It has been suggested (Armitage, Livio & Pringle 2001; Zhu, Hartmann & Gammie 2009) that this may explain FU Orionis outbursts. Self-gravity will transport mass to the inner disc where it will pile-up and cause the temperature in the inner disc to rise in order to remain gravitationally stable. Once hot enough for there to be partial ionisation, MRI will operate, rapidly draining the inner disc producing an FU Orionis-like outburst event.

### 2.4 Numerical method

We consider an initial core mass,  $M_c$ , with angular velocity,  $\Omega_c$  and choose initially a small timestep,  $dt$ . The disc is modelled by a grid with 500 logarithmically spaced grid points extending from  $r_{in} = 0.25$  au to  $r_{out} = 10a_o$ . This does mean that the grid spacing is not the same for different values of  $\Omega_c$ , but does ensure that the outer edge of the disc should never reach the outer edge of the grid. The initial infall is modelled as described in Section 2.1 and we assume that any material that falls inside the inner edge of the disc falls directly onto the protostar. After the first small timestep we then have a small amount of mass on the protostar, and the rest of the material distributed throughout the disc as described by equation (2). This means we now know the disc surface density,  $\Sigma$ . The midplane temperature,  $T_c$ , is then determined using  $Q = 2$  with the additional constraint that  $T_c \geq 10$  K. The optical depth,  $\tau$ , cooling time,

$t_{\text{cool}}$ , and effective gravitational viscosity,  $\nu_g = \alpha_g c_s^2 / \Omega$ , can then be determined and the disc is evolved using equation (4). The amount of mass accreting onto the star is determined from the difference between the disc mass before and after viscous evolution. The new mass distribution in the disc also changes the gravitational potential resulting in a lack of force balance in the disc. To achieve force balance material is moved inwards using the method described in Bath & Pringle (1981). The infall is then repeated with again some mass falling directly onto the protostar and the rest being distributed throughout the disc. However, when adding mass to the disc, the added material will generally have a lower specific angular momentum than the material already in the disc. This gives rise to an inflow which we take into account using, again, the method described by Bath & Pringle (1981). This once again changes the gravitational potential and so the lack of force balance must also be accounted for as before. The new disc surface density can then be used to recalculate the new gravitational viscosity and the process is repeated.

After the initial timestep (in which we essentially populate the disc with a small amount of mass), the subsequent timesteps are determined after the viscosity has been calculated and are set to be a small fraction of the smallest diffusion time across a grid cell. We use a zero-torque boundary,  $\Sigma(r_{\text{in}}) = 0$ , at the inner edge of the grid and although the outer boundary has no influence on the results, we set  $v_r = 0$  at this location.

### 3 RESULTS

We consider core masses from  $0.25 M_{\odot}$  to  $5 M_{\odot}$ . In all cases we choose the radius of the cloud such that the resulting uniform density of  $\rho = 6 \times 10^{-19} \text{ g cm}^{-3}$  gives a free-fall time,  $t_{\text{ff}}$ , of 86900 years. For  $M_c = 1 M_{\odot}$  this corresponds to a radius of 0.03 pc. The angular velocity is parametrised using  $f = \Omega_c / \sqrt{G\rho_c}$  and we vary  $f$  from  $f = 0.05$  to  $f = 1.3$ , corresponding to angular velocities between  $1.6 \times 10^{-15} \text{ rad s}^{-1}$  and  $2.6 \times 10^{-13} \text{ rad s}^{-1}$ . In many situations, the angular velocity is represented as the ratio of the total kinetic energy of rotation to the absolute value of the gravitational potential energy, often referred to as  $\beta$ . The relationship between  $\beta$  and  $f$  is  $\beta = f^2 / (2\pi)$  and so our chosen rotation rates correspond to  $\beta$  values between  $\beta = 0.0004$  and  $\beta = 0.27$ .

#### 3.1 Quasi-steady evolution

It has been suggested (Rice & Armitage 2009) that a self-gravitating protoplanetary disc will settle into a quasi-steady state with a mass transfer rate that is approximately the same at all radii. Rice & Armitage (2009), however, assumed initial power-law surface density profiles which were evolved until a quasi-steady state was achieved. Here, we self-consistently build and evolve the disc through the collapse of a uniform density molecular cloud core. Figure 1 shows the disc properties at  $t = t_{\text{ff}}$ ,  $t = 2t_{\text{ff}}$ , and  $t = 5t_{\text{ff}}$  for  $M_c = 1 M_{\odot}$  and for  $f = 0.1$ . Each panel shows the disc surface density (solid line), central temperature (dash-dot-dot-dot line), effective gravitational  $\alpha$  (dash-dot line), and mass accretion rate (dashed line) all plotted against radius

from 0.25 au to 200 au. The left-hand y-axis is scaled for surface density and temperature, while the right-hand y-axis is scaled for  $\alpha_g$  and mass accretion rate. The mass accretion rate is determined using  $\dot{M} = 3\pi\nu\Sigma$  (Pringle 1981). Figure 2 is the same as Figure 1 except that  $f = 0.8$  (i.e., the initial core rotation rate is faster in Figure 2 than in Figure 1).

As suggested by Rice & Armitage (2009), the disc quickly settles into a quasi-steady state with a mass transfer rate that, apart from the very inner disc, is similar at all radii. The low mass transfer rate in the inner disc is due to the assumption that MRI operates when  $T_c > 1400 \text{ K}$  (Zhu, Hartmann & Gammie 2009), which we approximate by setting  $\alpha = \alpha_{\text{ss}} + \alpha_g = 0.01$  when this condition is satisfied. The disc therefore has short, episodic periods of rapid accretion (not shown in Figure 1 or Figure 2) draining mass from the inner disc, and much longer quiescent periods while the inner disc is replenished. We don't, however, claim that we are modelling the processes in the inner disc particularly accurately. A much more detailed analysis has been carried out by Zhu et al. (2009).

For  $f = 0.1$  (Figure 1, the disc is quite compact due to the slow rotation producing a small  $a_{\text{max}}$ . The disc does expand slightly with time, reaching an outer radius of  $\sim 100$  au at  $t = 5t_{\text{ff}}$ . For  $f = 0.8$  (Figure 2) the disc radius is much larger and actually extends initially beyond the 200 au shown in Figure 2. In both cases, the disc properties are, however, essentially the same as shown by Rice & Armitage (2009) and remain largely unchanged over the 5 free-fall times shown in both Figure 1 and Figure 2. In this quasi-steady state, the disc has a reasonably steep surface density profile ( $\Sigma \propto r^{-1.5}$ ). The  $\alpha$  values, on the other hand can increase dramatically with radius due to the optically thick inner disc resulting in a very long cooling times - and hence small  $\alpha$  values - and the optically thin outer disc resulting in short cooling times and large  $\alpha$  values.

The surface density profile is also not a pure power-law, and has a significant fraction of the mass in the inner disc ( $r < 10$  au). The form of the surface density profile can be largely understood from the temperature profile. In the outer disc, the temperature is limited by our assumed minimum of 10 K. The temperature rises with decreasing radius, eventually reaching the temperature ( $T_c = 170 \text{ K}$ ) above which ice mantles can no longer exist on the solid grains, generally known as the ice- or snowline. This produces an abrupt change in the opacity, the local cooling time, and consequently the effective gravitational viscosity. The tendency to evolve to a state with roughly constant  $\dot{M}$  then produces a corresponding change in the surface density profile. The temperature then continues to rise with decreasing radius, eventually reaching 1400 K and becoming sufficiently ionised for MRI to operate. This sets an effective maximum temperature and also produces a subtle change in the surface density profile. A detailed description of how the surface density and temperature profiles vary in the different opacity regimes is included in Clarke (2009).

Not only does the quasi-steady nature of the disc persist for a number of free-fall times, it is also qualitatively the same for all our chosen parameters. Figure 3 shows the disc properties (as in Figure 1 and Figure 2) at  $t = t_{\text{ff}}$  for  $f = 0.8$  and for  $M_c = 0.5 M_{\odot}$  (top panel) and  $M_c = 5 M_{\odot}$  (bottom panel). The form of the profiles is essentially the same as in Figures 1 and 2. A few quantitative differences are that

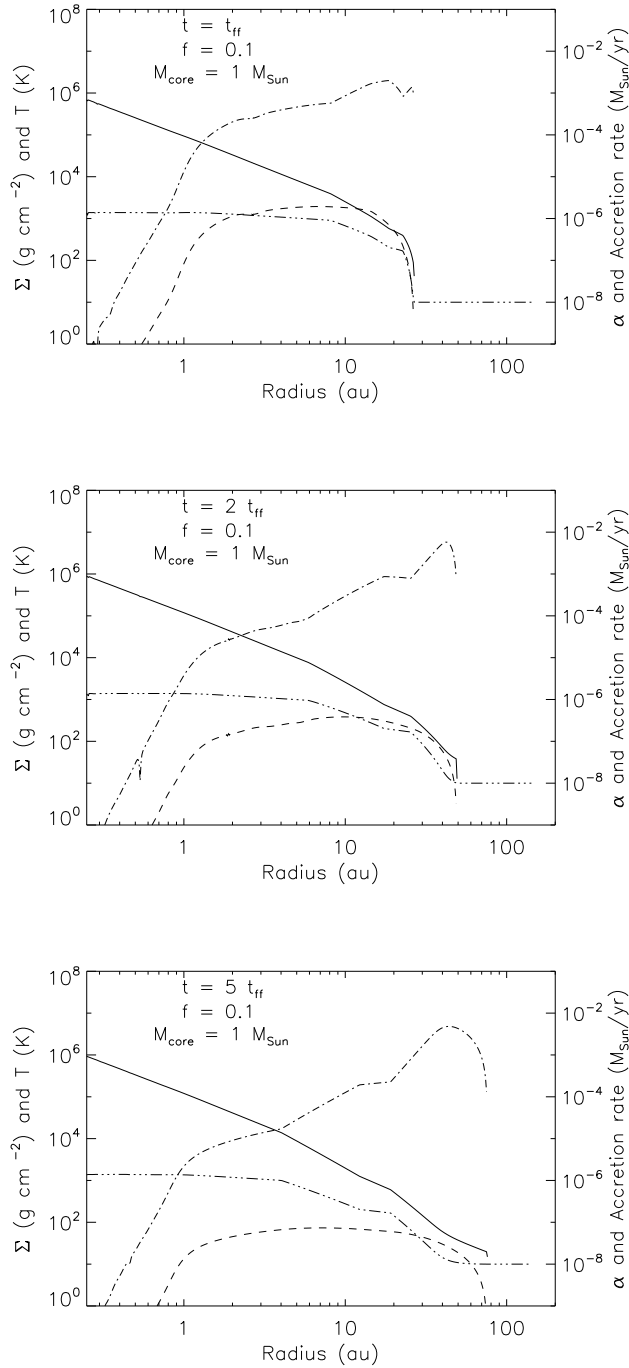


**Figure 1.** Disc properties for  $M_{\text{core}} = 1 M_{\odot}$  for  $f = 0.1$  at  $t = t_{\text{ff}}$ ,  $t = 2t_{\text{ff}}$ ,  $t = 5t_{\text{ff}}$ . Each panel shows the surface density  $\Sigma$ , (solid line), temperature (dash-dot-dot line), effective gravitational  $\alpha$  (dash-dot line), and mass accretion rate (dashed line). The left-hand y-axis is for  $\Sigma$  and temperature, while the right-hand y-axis is for  $\alpha$  and mass accretion rate. This figure illustrates that the disc quickly settles into a quasi-steady state that persists for many free-fall times.

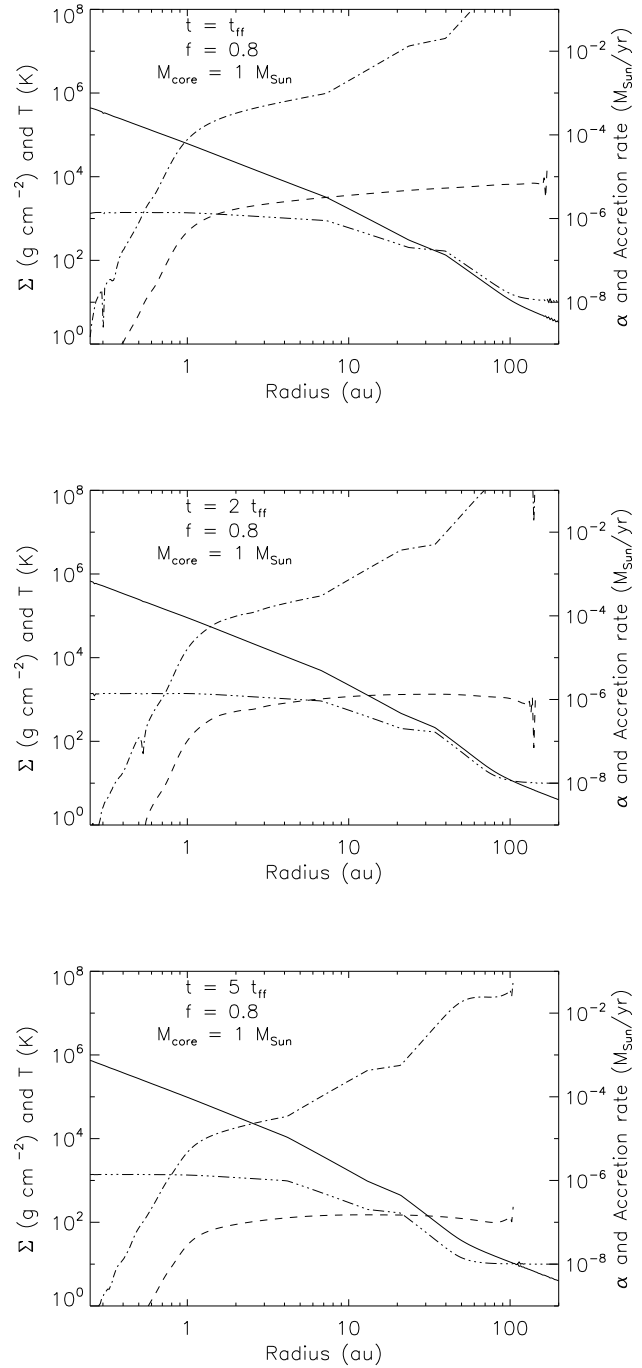


**Figure 2.** The same as in Figure 1 except for  $f = 0.8$ . This again shows that the disc settles into a quasi-steady state that persists for many free-fall times.

the surface density, the radius of the ice/snowline, and the radial extent of the region over which MRI can operate all increase with increasing core mass. Figure 2 also illustrates how the snowline moves in with time starting at  $\sim 50$  au when  $t = t_{\text{ff}}$  and moving in towards 10 au at  $t = 5t_{\text{ff}}$ .

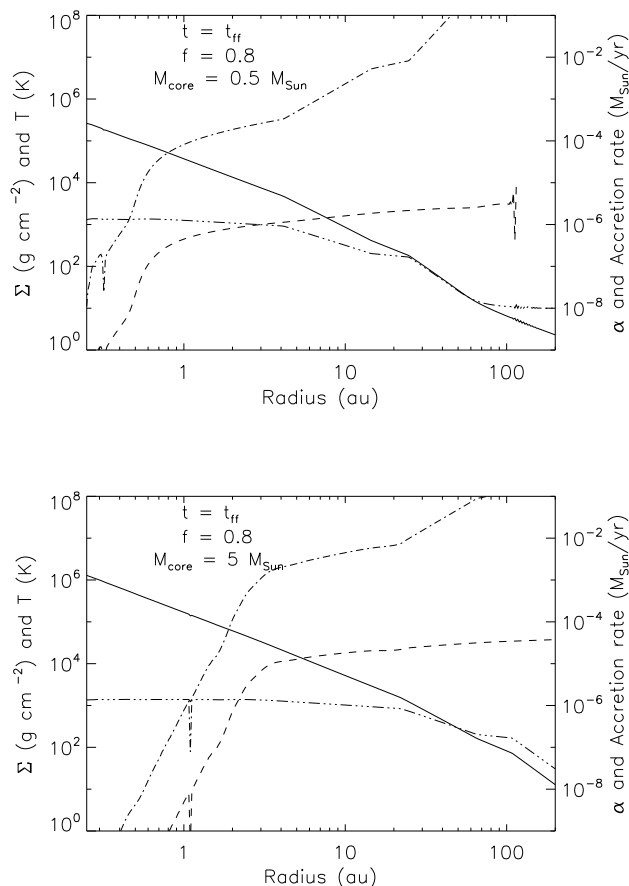


**Figure 3.** Disc properties for  $f = 0.8$  and for  $M_{\text{core}} = 0.5 M_{\odot}$  (top panel) and  $M_{\text{core}} = 5 M_{\odot}$ . This figure illustrates that the quasi-steady nature of self-gravitating discs is largely the same for all core masses. There are some quantitative differences such as the surface density, the radius of the ice/snowline, and the radial extent over which MRI can operate all increase with increasing core mass.

### 3.2 Mass accretion rates

We compute the accretion rate onto the protostar by simply determining how its mass changes with time. The disc accretion rate is computed using  $\dot{M} = 3\pi\nu\Sigma$  measured at a fixed location in the disc (generally 3 au for slowly rotating cores and 10 au for rapidly rotating cores). Figure 4 shows how the disc accretion rate (dashed-line) and protostar accretion rate vary with time for  $M_c = 1 M_{\odot}$  and for  $f = 0.1$  (top panel) and  $f = 0.8$  (bottom panel). In both cases shown the protostar accretion rate rises rapidly with time and peaks at  $t \sim t_{\text{ff}}$  ( $\sim 10^5$  years). It then drops significantly over the next freefall time and then changes more slowly from  $t = 2t_{\text{ff}}$  to  $t = 1$  Myr. The protostar accretion rate also becomes quite variable after  $t = 2t_{\text{ff}}$  due to the accretion onto the protostar occurring episodically when  $T_c > 1400$  K. In fact the protostar accretion rate has been averaged over  $0.1t_{\text{ff}}$  and so the variability that our model produces is somewhat more extreme than shown in Figure 4, although we don't claim to be modelling this variability particularly accurately.

The disc accretion rate (dashed line) is much smoother than the protostar accretion rate and, in Figure 4, has not been averaged. This illustrates that the disc is able to reach a quasi-steady state on timescales much shorter than the freefall time. What Figure 4 also shows is that for rapidly rotating cores (large  $f$ ) the accretion onto the core is governed by accretion through the disc, while for slowly rotating cores the protostar grows initially through direct infall and only after infall ceases ( $t > 2t_{\text{ff}}$ ) does disc accretion determine the rate at which mass is accreted onto the protostar. The accretion rate at  $t = 1$  Myr also depends on the core rotation and increases with increasing  $f$ . From Figures 1, 2 and 3, it is clear that the surface density profiles do not vary significantly with  $f$  or with time. What is different is the mass of the central protostar. The protostar mass increases with decreasing  $f$  and consequently (since we assume  $Q = 2$ ) produces disc temperatures that also decrease with decreasing  $f$ . This means that the cooling rate, effective gravitational viscosity, and consequently the disc accretion rate all decrease with decreasing  $f$ . In fact for very slow rotating cores ( $f < 0.08$ ) it is difficult to sustain disc accretion beyond a few freefall times.

Since we have carried out a large number of simulations with various core masses and with various rotation rates, we can consider how the mass accretion rate varies with protostar mass during the first 1 Myr. Figure 5 shows the mass accretion rate against protostar mass from our simulations (solid dots) compared with observed accretion rates for T Tauri stars taken from Gullbring et al. (1998), White & Ghez (2001), Calvet et al. (2004), and Natta, Testi & Randich (2006). The data points from our simulations are at  $t = t_{\text{ff}}$  (the peak accretion rate) and then at 50 randomly chosen times between  $t = t_{\text{ff}}$  and  $t = 1$  Myr. The reasonably sparsely populated upper region illustrates how the accretion rate drops, within about a freefall time, to a value an order of magnitude or more lower than the peak value. The lower region is more densely populated, making it more likely that observed accretion rates would fall in this band. This likelihood is increased further due to the system being more heavily embedded during the first few freefall times, making it harder to measure accurate accretion rates at these early times.

The accretion rates from the simulations don't compare particularly well with the observed accretion rates (open circles), with the observed accretion rates tending to be lower than the those from the simulations. The observed systems are, however, probably at a later stage of evolution than the simulated systems. The highest observed accretion rates are, however, consistent with what we would expect for the youngest systems, suggesting that self-gravitating transport can dominate until the earliest stages of the T Tauri phase. It has also been suggested that the accretion rate should vary approximately with mass as  $\dot{M} \propto M^2$  (Muzerolle et al. 2005; Natta, Testi & Randich 2006). The upper boundary of our simulated accretion rates, however, has a mass dependence closer to  $\dot{M} \propto M$  (illustrated by the solid line in Figure 5) and is consistent with that suggested by Vorobyov & Basu (2009) and with the upper envelope of observed accretion rates (Hartmann et al. 2006). That the observed accretion rates are for protostars of various ages will introduce a scatter that could result in what appears to

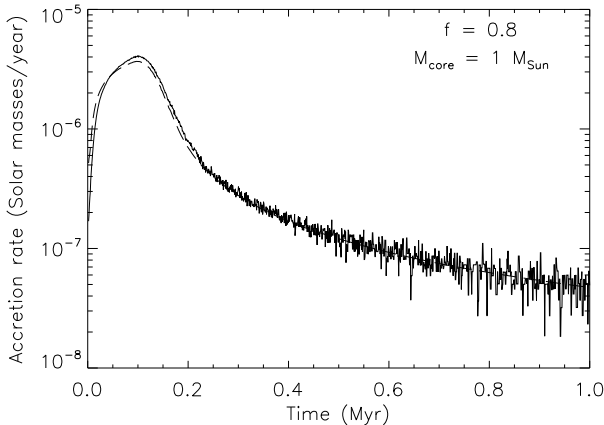
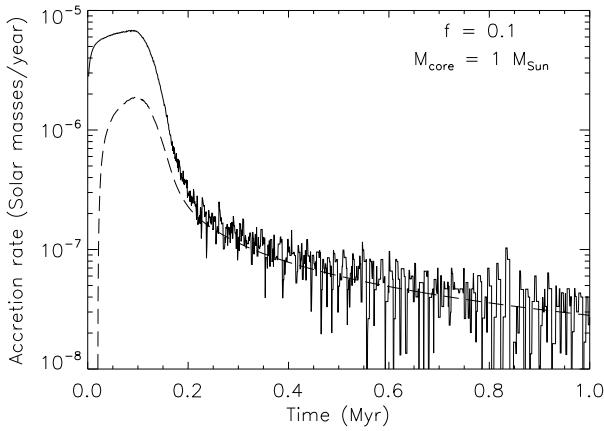


**Figure 4.** Figure showing the accretion rate onto the protostar (solid line) and through the disc (dashed line) for  $M_{\text{core}} = 1 M_{\odot}$  and  $f = 0.1$  (top panel) and  $f = 0.8$  (bottom panel). The accretion rate initially increases with time, peaking at  $t \sim t_{\text{ff}}$ . The accretion onto the protostar is also quite variable and in fact has been averaged over  $0.1t_{\text{ff}}$  so is actually more variable than shown. The disc accretion is, however, much steadier and illustrates the quasi-steady nature of the disc evolution. The figure also shows that for high core rotation rates ( $f = 0.8$ ) accretion onto the protostar is governed by accretion through the disc, while for slow core rotation rates ( $f = 0.1$ ) the protostar grows primarily through direct infall during the first 2 free-fall times.

be a steeper dependence on protostar mass than is actually the case.

### 3.3 Disc fragmentation

It has been proposed (Boss 1998, 2002) that discs that are sufficiently gravitationally unstable could fragment to produce bound objects and that these bound objects could subsequently contract to form either gas giant planets or brown dwarf stars. What is now well known is that disc fragmentation requires rapid cooling (Gammie 2001; Rice et al. 2003) and that there is a minimum cooling time - which may depend on the actual cooling function (Cossins, Lodato & Clarke 2009) - for which a self-gravitating disc can remain in a quasi-steady state with-

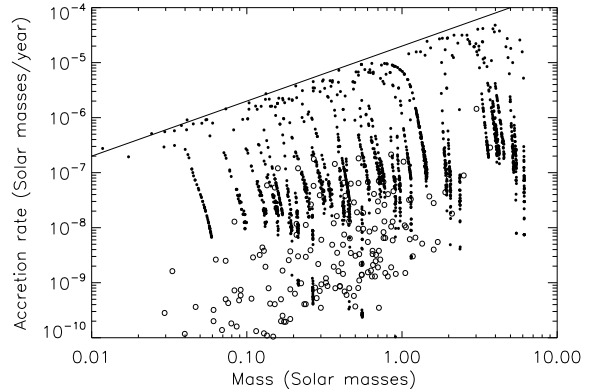


**Figure 5.** Protostar accretion rates plotted against protostar mass from all our simulations (solid dots). The data points are at  $t = t_{\text{ff}}$  and at 50 random chosen times between  $t = t_{\text{ff}}$  and 1 Myr. The sparsely populated region at the top illustrates how the accretion rate drops rapidly between  $t = t_{\text{ff}}$  and  $t = 2t_{\text{ff}}$  and suggests that we are not particularly likely to observe systems in this state. The open circles show observed accretion rates for T Tauri stars taken from Gullbring et al. (1998), White & Ghez (2001), Calvet et al. (2004), Natta, Testi & Randich (2006). Although these don't compare particularly well with our calculated accretion rates, the highest observed accretion rates are consistent with what we would expect for the youngest systems, and many of the observed systems are probably at a later stage of evolution than the simulated systems. The solid line shows that the peak of the simulated accretion rates depend linearly on protostar mass ( $\dot{M} \propto M$ ) and has the same relation as the upper envelope of the observed accretion rates (Hartmann et al. 2006).

out fragmenting. The relationship between effective gravitational  $\alpha_g$  and cooling time (see equation (12)) allows us to define the fragmentation boundary in terms of  $\alpha_g$ . It has been shown (Rice et al. 2005) that fragmentation occurs for  $\alpha_g > 0.06$  and that this boundary is independent of the specific heat ratio  $\gamma$ .

Figures 1, 2, and 3 show that in all cases, the  $\alpha_g$  values in the inner disc are well below that required for fragmentation ( $\alpha_g < 10^{-2}$ ), but that the outer parts of some discs could be susceptible to fragmentation. The requirement for fragmentation is that  $Q \sim 1$  and  $\alpha_g > 0.06$ . In our simulations we assume  $Q$  settles to  $Q = 2$ , so we don't quite satisfy the first condition, but we can at least identify the regions where the  $\alpha_g$  condition is satisfied and therefore where  $Q$  will decrease and fragmentation is most likely. Figure 6 shows the range of radii where fragmentation could occur at  $t = t_{\text{ff}}$  (triangles) and  $t = 1.5t_{\text{ff}}$  (diamonds), for various  $f$  values. Each vertical line is for a single core mass and we consider core masses of  $M_c = 0.25 M_{\odot}$  (solid line),  $M_c = 0.5 M_{\odot}$  (dashed line),  $M_c = 1 M_{\odot}$  (dash-dot line),  $M_c = 2 M_{\odot}$  (dash-dot-dot-dot line), and  $M_c = 5 M_{\odot}$  (long dash line).

Figure 6 shows that only the outer disc (beyond  $\sim 40$  au) has conditions suitable for fragmentation, consistent with numerical simulations (Stamatellos et al. 2007) and possibly also with some observations (Greaves et al. 2008). The inner radius of the fragmentation zone increases with core mass and for a core mass of  $1 M_{\odot}$ , which produces a central protostar with a mass close to  $1 M_{\odot}$ , is  $60 - 70$  au,

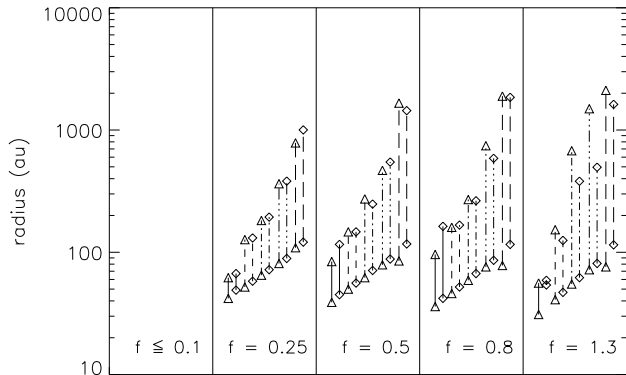


**Figure 6.** Figure showing the range of radii where fragmentation could occur (defined as the region where  $\alpha > 0.1$ ). We find that the fragmentation conditions are never satisfied when  $f \leq 0.1$  and are always satisfied when  $f \geq 0.25$ . To illustrate that the fragmentation conditions can be satisfied for many dynamical times, the fragmentation range is plotted at  $t = t_{\text{ff}}$  (triangles) and  $t = 1.5t_{\text{ff}}$  (diamonds). The core masses considered are  $M_{\text{core}} = 0.25 M_{\odot}$  (solid line),  $M_{\text{core}} = 0.5 M_{\odot}$  (dashed line),  $M_{\text{core}} = 1 M_{\odot}$  (dash-dot line),  $M_{\text{core}} = 2 M_{\odot}$  (dash-dot-dot line), and  $M_{\text{core}} = 5 M_{\odot}$  (long-dash line). The inner fragmentation radius increases with core mass from  $\sim 40$  au for  $M_{\text{core}} = 0.25 M_{\odot}$  to  $\sim 100$  au for  $M_{\text{core}} = 5 M_{\odot}$ . The radial range also increases with increasing core mass, but this should be interpreted cautiously as the outer disc could be susceptible to ionisation from cosmic rays that may stimulate MRI turbulence (Rafikov 2009) and stabilise these regions against fragmentation.

consistent with Clarke (2009). The radial range that can undergo fragmentation is quite small for low core masses (10 – 20 au for  $M_c = 0.25 M_{\odot}$ ) but increases dramatically with core mass. This result needs to be interpreted somewhat cautiously as the outer parts of these discs could be susceptible to ionization through cosmic rays that may stimulate MRI turbulence (Rafikov 2009) and stabilise these regions against fragmentation.

Although we can't really predict the possible masses of the objects that may form via fragmentation, Kratter, Murray-Clay & Youdin (2009) suggest that the initial fragmentation masses will be  $\sim 1 M_{\text{Jupiter}}$ . The large amount of mass in these outer regions, however, suggests that such fragments will continue to grow and that the isolation mass can easily be  $> 100 M_{\text{Jupiter}}$ . Fragmentation in the outer parts of these discs is therefore unlikely to form planetary mass objects and will probably form sub-stellar or stellar mass companions.

None of our simulations with  $f = 0.1$  or less had any regions susceptible to fragmentation. This was essentially due to these slow rotation rates producing compact discs with most of the mass in the optically thick inner disc and very little mass in the optically thin outer disc. It has been suggested (Miyama, Hayashi & Narita 1984) that fragmentation depends on both the ratio of the thermal to gravitational energy  $\xi$  and the ratio of the energy of rotation to the gravitational energy  $\beta = f^2/(2\pi)$ . Miyama, Hayashi & Narita (1984) find that fragmentation

occurs if  $\xi\beta < 0.12$ . If we assume an initially isothermal core, with sound speed  $c_s$ , then (see Walch et al. (2009))

$$\xi = \frac{2c_s^2 R_c}{GM_c}. \quad (13)$$

Since we assume all our cores have the same density and hence freefall time, the  $\xi$  values of our cores vary with core mass. Since fragmentation is possible for all core masses with  $f \geq 0.25$  and for none of the core masses when  $f \leq 0.1$ , this suggests that what primarily determines if a disc will fragment is the initial rotation rate of the cloud core. The reason for this is that, in our simulations, the discs very quickly settle into a quasi-steady state, with  $Q = 2$ , that is in thermal equilibrium. This quasi-steady state is essentially independent of the initial thermal properties of the core and depends largely on how much mass is in the system. If the initial rotation is such that some of this mass can be deposited in the outer, optically thin parts of the disc, then fragmentation is quite likely. Figure 6 also shows that the fragmentation region remains largely unchanged for at least  $0.5t_{\text{ff}}$  (from  $t = t_{\text{ff}}$  to  $t = 1.5t_{\text{ff}}$ ). We find, in fact, that conditions suitable for fragmentation actually persist for a freefall time or longer (which is many dynamical times even in the outer disc), but are generally no longer satisfied after  $\sim 2$  freefall times for the lower mass cores and after 3 – 4 freefall times for the higher mass cores.

### 3.4 Disc and protostar masses

Figure 7 shows the evolution of the disc and protostar masses against time for  $M_{\text{core}} = 1 M_{\odot}$  and for  $f = 0.1$  (top panel),  $f = 0.25$  (middle panel), and  $f = 0.8$  (bottom panel). In all cases, the solid line shows the evolution of the core mass, while the dashed lines show the disc mass within 10 au, 100 au, and the total disc mass. For  $f = 0.1$  the disc does not extend beyond 100 au and so the mass inside 100 au and the total disc mass are the same. The figure illustrates that as the core rotation rate increases, the core mass decreases and more and more mass is deposited at large radii ( $r > 100$  au). What these figures also illustrate is that the mass inside 10 au and the mass inside 100 is only weakly dependant on the rotation rate, again illustrating the quasi-steady nature of these discs.

Figure 8 is the same as Figure 7 except it is for  $f = 0.8$  and  $M_{\text{core}} = 0.5 M_{\odot}$  (top panel),  $M_{\text{core}} = 2 M_{\odot}$  (middle panel) and  $M_{\text{core}} = 5 M_{\odot}$  (bottom panel). It is clear from both Figure 7 and Figure 8 that in all cases, there is an epoch when the disc mass exceeds the mass of the central object. For small  $f$  values, this epoch is quite short ( $< 1t_{\text{ff}}$ ) while for larger  $f$  values, the disc may remain more massive than the central star for many freefall times. The outer parts ( $r > 50 - 100$  au) are, however, susceptible to fragmentation and may break up to produce companions. The inner parts ( $r < 100$  au) of these discs are only generally comparable in mass to the central protostar for  $t < 2t_{\text{ff}}$ . This does, however, suggest that our local approximation may not be strictly valid, and that the effective gravitational  $\alpha$  will not be determined by the local cooling rate. It has been suggested (Kratter, Matzner & Krumholz 2008; Vorobyov 2009) that there should be two self-gravitating  $\alpha$  parametrisations, one when the disc-to-star mass ratio is small, and the other when the disc-to-star mass ratio is large. This may be the case,



but we assume that even if the disc is massive relative to the central star, the system would still settle into a state with constant  $Q$  and be in thermal equilibrium. We don't know if, in such a state, the local dissipation rate will be set by the local cooling rate, but we assume that such an assumption is at least reasonable at this stage. The figures also illustrate that in a quasi-steady, self-gravitating state at least 50 % of the disc mass within 100 au is located inside 10 au. This large amount of mass in the inner disc could have implications for, and could aid, planet formation. Detecting such massive inner discs is, however, extremely difficult as they are very optically thick.

As discussed in the previous section, it is also likely that for  $f \geq 0.25$  the outer disc will be very unstable and may fragment to produce companions. The exact radius at which this occurs depends on the mass of the central star, but is typically between 60 and 100 au. A significant fraction of the material in the outer disc ( $r > 100$  au) is therefore likely to be converted into companions which will truncate the outer disc at a radius of 50 – 75 au, depending on where the fragmentation occurs. A standard way to determine disc masses observationally is to fit the mass by modelling the spectral energy distribution (SED) (Robitaille et al. 2006; Andrews et al. 2009). The results from such modelling can, however, be ambiguous (Eisner et al. 2005) and, in particular, a lot of mass can be hidden in optically thick regions of the disc. The enhanced mass in the optically thick inner 10 au should therefore not contribute significantly to the SED, and the discs in Figures 7 and 8 would consequently appear to have a mass - determined through SED modelling - roughly equal to the difference between the mass within 100 au and the mass inside 10 au. For T Tauri-like protostar masses (e.g., Figure 7), this would be 0.1 – 0.2  $M_{\odot}$  consistent with that obtained for class I sources (Eisner et al. 2005).

If we only consider the disc mass within 100 au, since the outer disc is likely to be removed through fragmentation, Figure 8 and the bottom panel of Figure 7 also shows that the disc-to-protostar mass ratio increases with decreasing protostar mass, consistent with observations in the Orion Nebula cluster that massive discs are more common around lower-mass stars (Eisner et al. 2008). For core masses below  $\sim 1 M_{\odot}$ , however, the disc mass is very similar to the mass of the central star and again brings into question our assumption that the transport through self-gravity can be treated as a local process. The inner fragmentation radius for these lower-mass cores (see Figure 6) is, however, also closer to 50 au than 100 au potentially converting more of the mass in the disc into companions. The relatively low disc-to-star mass ratio for protostars with masses above a few solar masses may also help to explain why most discs around relatively massive stars disappear on much shorter timescales than discs around solar-like T Tauri stars.

### 3.5 Additional sources of viscosity

The discussion in the section above suggests that fragmentation in the outer disc and the presence of an optically thick inner disc may result in very young protostars with T Tauri-like masses appearing to have disc masses comparable to that observed. Figure 5 and Figure 4, however, show that at  $t = 1$  Myr, the accretion rates around these protostars is between  $10^{-8}$  and  $10^{-7} M_{\odot} \text{ yr}^{-1}$ . At this rate,

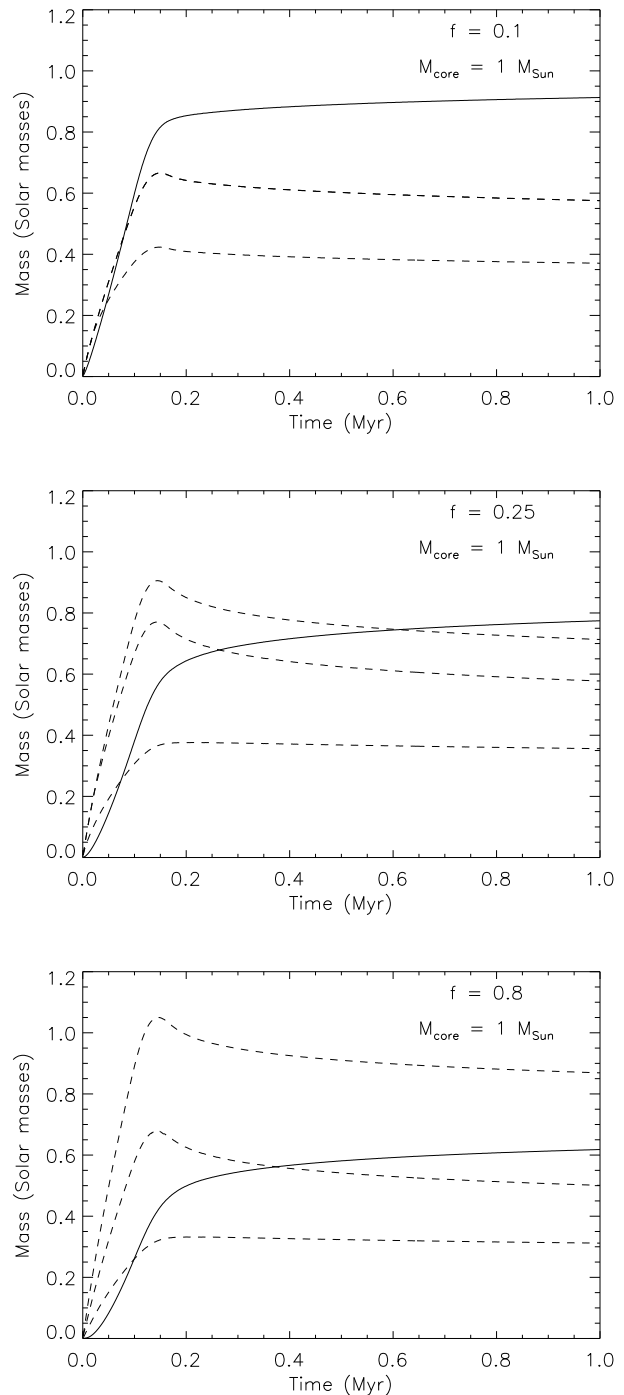


**Figure 7.** Protostar (solid line) and disc (dashed lines) masses plotted against time for  $M_{\text{core}} = 1 M_{\odot}$  and for  $f = 0.1$  (top panel),  $f = 0.25$  (middle panel), and  $f = 0.8$  (bottom panel). The different dashed lines show the disc mass inside 10 au, 100 au, and the total disc mass. The figure illustrates that as the core rotation rate increases, the core mass decreases and more and more mass is deposited at large radii in the disc. The figure shows that in all cases a significant fraction ( $\sim 50\%$ ) of the mass inside 100 au is located in the optically thick inner 10 au.

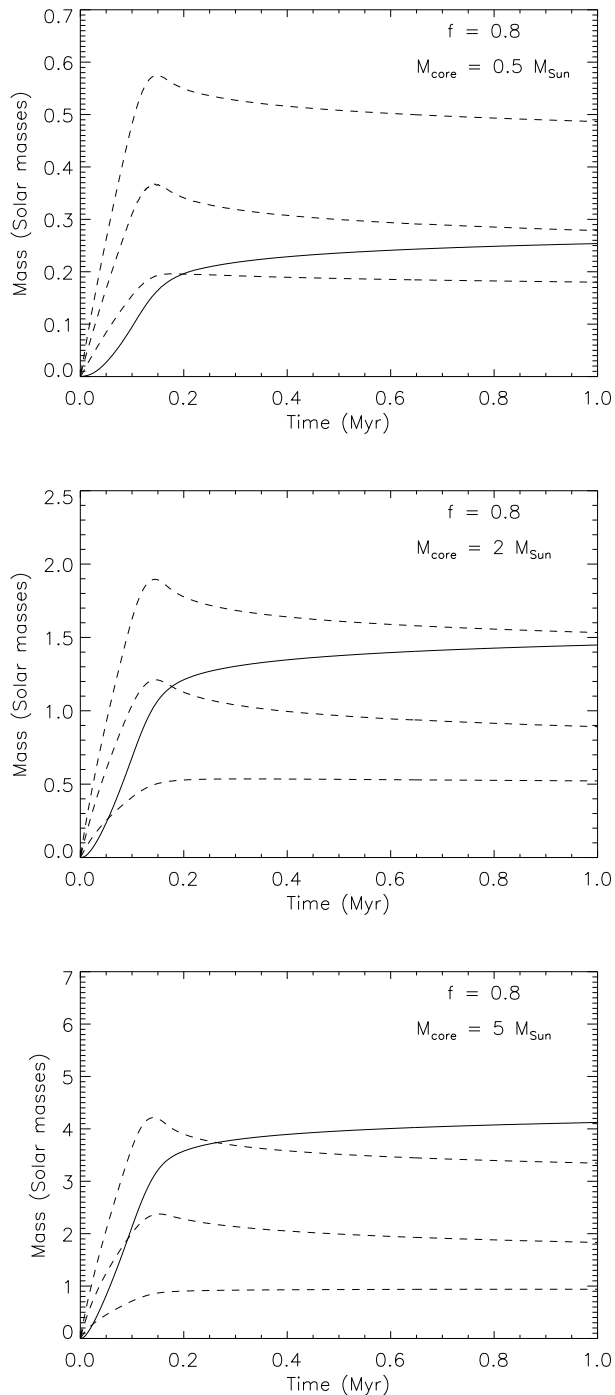


**Figure 8.** Protostar (solid line) and disc (dashed lines) masses plotted against time for  $f = 0.8$  and for  $M_{\text{core}} = 0.5 M_{\odot}$  (top panel),  $M_{\text{core}} = 2 M_{\odot}$  (middle panel), and  $M_{\text{core}} = 5 M_{\odot}$ . The different dashed lines show the disc mass inside 10 au, 100 au, and the total disc mass. The figure shows that a significant fraction ( $\sim 50\%$ ) of the mass inside 100 au is located in the optically thick inner 10 au. Considering only the disc mass inside 100 au (since the outer disc is potentially susceptible to fragmentation) the disc-to-protostar mass ratio decreases with increasing core mass which is consistent with observations in the Orion Nebula cluster (Eisner et al. 2008), and could help to explain why discs around relatively massive stars disappear on much shorter timescales than discs around lower-mass T Tauri stars.

removing the final disc material ( $M_{\text{disc}} > 0.3 M_{\odot}$  within 100 au according to Figures 7 and 8) would take in excess of  $10^7$  yrs. This is significantly longer than the disc dispersal timescale of  $\sim 5$  Myr suggested by observations of disc fractions in star forming regions of different ages (Haisch, Lada & Lada 2001). Rice & Armitage (2009) have also shown that the mass accretion rate also drops dramatically with disc mass, becoming very small for disc masses less than a tenth of the protostar mass. If self-gravity is the only transport mechanism then the timescale for removing the disc material would be much longer than observed. This suggests that there should be an additional transport mechanism. The most likely candidate is MRI operating in the upper layers of the disc (Gammie 1996).

#### 4 DISCUSSION AND CONCLUSIONS

We consider here the evolution of protostellar discs that form through the collapse of molecular cloud cores and in which the primary transport mechanism is self-gravity. We assume that the discs settle quickly into a marginally gravitationally stable state with  $Q = 2$  and are then in thermal equilibrium. In this state angular momentum transport is driven by an effective gravitational viscosity that is calculated using the assumption that energy is dissipated at a rate equal to the rate at which the disc loses energy through radiative cooling. Following the work of Armitage, Livio & Pringle (2001) and Zhu, Hartmann & Gammie (2009) we also assume that MRI (Balbus & Hawley 1991) will operate if the disc is hot enough ( $T > 1400$  K) to be partially ionised. This occurs only in the inner disc and is episodic - draining material from the inner disc and then turning off until the inner disc has been replenished by material from the outer disc - and has therefore been proposed as a mechanism for explaining FU Orionis outbursts (Hartmann & Kenyon 1996).

Our simulations consider a range of cores masses ( $0.25 - 5 M_{\odot}$ ) and a range of rotation rates ( $0.05 \leq f \leq 1.3$  with  $f = \Omega_c / \sqrt{G\rho_c}$ ). The primary results are as follows

- The discs settle quickly into a quasi-steady state with a reasonably steep surface density profile and with a lot ( $\sim 50\%$ ) of the mass within 100 au located inside 10 – 20 au. The disc-to-star mass ratio decreases with increasing protostar mass, consistent with observations in the Orion Nebula cluster (Eisner et al. 2008). Although the disc masses tend to be higher than observed, with so much mass located in the inner optically thick regions of the disc, most of this mass would be difficult to detect with current techniques.
- Although the mass accretion rates are initially higher than those observed, these high accretion rates only persist for  $\sim 1$  free-fall time and quickly drop to values similar to that observed. The simulations also suggest that the accretion rate varies less strongly with protostar mass ( $\dot{M} \propto M_*$ ) than suggested by observations ( $\dot{M} \propto M_*^2$ ) (Muzerolle et al. 2005; Natta, Testi & Randich 2006), but is consistent with the upper boundary of the observed accretion rates (Hartmann et al. 2006).
- In none of our simulations did the inner disc ( $r < 40$  au) have conditions suitable for fragmentation ( $\alpha_g > 0.06$ ). In some cases, the outer disc was susceptible to fragmentation, with the primary factor determining if a disc could fragment being the rotation rate of the molecular core.

The large amount of mass in these discs, however, suggests that fragmentation is more likely to result in sub-stellar or stellar companions than planetary mass objects (Kratte, Murray-Clay & Youdin 2009). None of our simulations with  $f \leq 0.1$  satisfied the fragmentation conditions while it was satisfied for all those with  $f \geq 0.25$ . The inner radius of the fragmentation region increased from  $\sim 40$  au for  $M_{\text{core}} = 0.25 M_{\odot}$  to  $\sim 100$  au for  $M_{\text{core}} = 5 M_{\odot}$  as did the radial range over which fragmentation could occur, although the outer regions of some of these discs could be stabilised against fragmentation by cosmic ray ionisation (Rafikov 2009).

- The mass accretion rate depends strongly on the disc mass and in all cases drops below  $10^{-7} M_{\odot} \text{ yr}^{-1}$  when the disc mass is still quite substantial ( $M_{\text{disc}} > 0.3 M_{\odot}$ ). If self-gravity were to remain the primary transport mechanism, disc clearing timescales would be significantly longer than that observed. This suggests that an additional transport mechanism, such as MRI occurring in the upper layers of the disc (Gammie 1996), must also operate. We propose that this additional mechanism is likely to be negligible initially and become more effective with time. This is probably the case for layered accretion which should become more efficient as the disc mass decreases and is consistent with the requirement that small dust grains must be depleted before MRI can operate effectively (Sano et al. 2000; Sano & Stone 2002; Ilgner & Nelson 2006), but the pile-up of material in the inner regions of the disc (ultimately resulting in episodic FU Orionis-like outbursts) would also not occur if the additional transport mechanism were too efficient at early times.

Ultimately it appears that transport driven by self-gravity can explain protostar formation and disc evolution at early times. Our simulations suggest that disc masses may - at early times - be higher than suggested by observations but these large disc masses also suggest that an additional transport mechanism must dominate at later times ( $t > 1$  Myr) to remove the remaining disc material within observed disc lifetimes. The pile-up of material in the inner regions of the disc - which may explain FU Orionis outburst - may also play an important role in the subsequent formation of planets.

## ACKNOWLEDGEMENTS

P.J.A. acknowledges support from the NSF (AST-0807471), from NASA's Origins of Solar Systems program (NNX09AB90G), and from NASA's Astrophysics Theory and Fundamental Physics program (NNX07AH08G). W.K.M.R. acknowledges support from the Scottish Universities Physics Alliance (SUPA). The authors would also like to thank the Isaac Newton Institute for Mathematical Sciences for their hospitality during the Dynamics of Discs and Planets Programme, and would like to acknowledge useful discussions with Lee Hartmann, Dick Durisen, Giuseppe Lodato and Neal Turner.

## REFERENCES

Andrews S.M., Wilner D.J., Hughes A.M., Chunhua Q., Dullemond C.P., 2009, *ApJ*, 700, 1502

Armitage P.J., Livio M., Pringle J.E., 2001, *MNRAS*, 324, 705  
 Balbus S.A., Hawley J.F., 1991, *ApJ*, 376, 214  
 Balbus S.A., Papaloizou J.C.B., 1999, *ApJ*, 521, 650  
 Bath G., Pringle J.E., 1981, *MNRAS*, 194, 962  
 Bell K.R., Lin D.N.C., 1994, *ApJ*, 427, 987  
 Blaes O.M., Balbus S.A., 1994, *ApJ*, 421, 163  
 Boley A.C., Mejía A.C., Durisen R.H., Cai K., Pickett M.K., D'Alessio P., 2006, 651, 517  
 Boss A.P., 1998, *ApJ*, 503, 923  
 Boss A.P., 2002, *ApJ*, 576, 462  
 Calvet N., Muzerolle J., Briceño C., Fernández J., Hartmann L., Saucedo J. L., Gordon K. D., 2004, *AJ*, 128, 1294  
 Caselli P., Benson P.J., Myers P.C., Tafalla M., 2002, *ApJ*, 572, 238  
 Cassen P.M., Moosman A., 1981, *Icarus*, 48, 353  
 Clarke C.J., 2009, *MNRAS*, 396, 1066  
 Cossins P., Lodato G., Clarke C., 2009, *MNRAS*, in press  
 Durisen R.H., Boss A.P., Mayer L., Nelson A.F., Quinn T., Rice W.K.M., 2007, in Reipurth B., Jewitt D., Keil K., eds, *Protostars and Planets V*. University of Arizona Press, Tucson, p701  
 Eisner J.A., Hillenbrand L.A., Carpenter J.M., Wolf S., 2005, *ApJ*, 635, 396  
 Eisner J.A., Plambeck R.L., Carpenter J.M., Corder S.A., Qi C., Wilner D., 2008, *ApJ*, 683, 304  
 Forgan D., Rice K., Stamatellos D., Whitworth A., 2009, *MNRAS*, in press  
 Gammie C.F., 1996, *ApJ*, 457, 355  
 Gammie C.F., 2001, *ApJ*, 553, 174  
 Greaves J.S., Richards A.M.S., Rice W.K.M., Muxlow T.W.B., 2008, *MNRAS*, 391, L74  
 Gullbring E., Hartmann L., Briceño C., Calvet N., 1998, *ApJ*, 492, 323  
 Haisch K.E., Lada E.A., Lada C.J., 2001, *AJ*, 121, 2065  
 Hartmann L., D'Alessio P., Calvet N., Muzerolle J., 2006, *ApJ*, 648, 484  
 Hartmann L., Kenyon S.J., 1996, *ARA&A*, 34, 207  
 Hubeny I., 1990, *ApJ*, 351, 632  
 Ilgner M., Nelson R.P., 2006, *A&A*, 445, 205  
 Johnson B.M., Gammie C.F., 2003, 597, 131  
 Kratter K.M., Matzner C.D., Krumholz M.R., 2008, *ApJ*, 681, 375  
 Kratter K.M., Murray-Clay R.A., Youdin A.N., 2009, *ApJ*, submitted  
 Larson R.B., 1969, *MNRAS*, 145, 271  
 Laughlin G., Bodenheimer P., 1994, *ApJ*, 436, 335  
 Lin D.N.C., Pringle J.E., 1990, *MNRAS*, 358, 515  
 Lin D.N.C., Pringle J.E., 1987, *MNRAS*, 225, 607  
 Lodato G., Rice W.K.M., 2004, *MNRAS*, 351, 630  
 Lodato G., Rice W.K.M., 2005, *MNRAS*, 358, 1489  
 Lynden-Bell D., Pringle J.E., 1974, *MNRAS*, 168, 603  
 Matzner C.D., Levin Y., 2005, *ApJ*, 628, 817  
 Mejía A.C., Durisen R.H., Pickett M.K., Cai K., 2006, *ApJ*, 619, 1098  
 Miyama S.M., Hayashi C., Narita S., 1984, *ApJ*, 279, 621  
 Muzerolle J., Luhmann K.L., Briceño C., Hartmann L., Calvet N., 2005, *ApJ*, 625, 906  
 Natta A., Testi L., Randich S., 2006, *A&A*, 452, 245  
 Papaloizou J.C.B., Nelson R.P., 2003, *MNRAS*, 339, 983  
 Pringle J.E., 1981, *ARA&A*, 19, 137  
 Rafikov R.R., 2005, *ApJ*, 621, L69  
 Rafikov R.R., 2009, *ApJ*, submitted.  
 Rice W.K.M., Armitage P.J., 2009, *MNRAS*, 396, 2228  
 Rice W.K.M., Armitage P.J., Bate M.R., Bonnell I.A., 2003, *MNRAS*, 339, 1025  
 Rice W.K.M., Lodato G., Armitage P.J., 2005, *MNRAS*, 364, L56

- Robitaille T.P., Whitney B.A., Indebetouw R., Wood, K.,  
Denzmore P., 2006, *ApJS*, 167, 256
- Sano T., Miyama S., Umebayashi T., Nakaon T., 2000, *ApJ*,  
543, 486
- Sano T., Stone J., 2002, *ApJ*, 577, 534
- Shakura N.I., Sunyaev R.A., 1973, *A&A*, 24, 337
- Stamatellos D., Whitworth A.P., Bisbas T., Goodwin S., 2007,  
*A&A*, 475, 37
- Stamatellos D., Whitworth A.P., 2008, *A&A*, 480, 879
- Terebey S., Shu F.H., Cassen P., 1984, *ApJ*, 286, 529
- Terquem C.E.J.M.L.J., 2008, *ApJ*, 689, 532
- Toomre A., 1964, *ApJ*, 139, 1217.
- van Boekel R., et al., 2004, *Nature*, 432, 479
- Vorobyov E.I., 2009, *New Astron.*, 15, 24
- Vorobyov E.I., Basu S., 2009, *ApJ*, in press
- Vorobyov E.I., Basu S., 2007, *MNRAS*, 381, 1009
- Walch S., Burkert A., Whitworth A., Naab T., Gritschneider M.,  
2009, *MNRAS*, in press.
- White R.J., Ghez A., 2001, *ApJ*, 556, 265
- Whitworth A.P., Stamatellos D., 2006, 458, 817
- Zhu Z., Hartmann L., Gammie C.F., 2009, *ApJ*, 694, 1045
- Zhu Z., Hartmann L., Gammie C., McKinney J.C., 2009, *ApJ*,  
701, 620